β decay of ^{40,42}S and ^{43}Cl

J. A. Winger,[1,*] P. F. Mantica,[2,3] and R. M. Ronningen[3]
[1]*Department of Physics and Astronomy, Mississippi State University, Mississippi State, Mississippi 39762, USA*
[2]*Department of Chemistry, Michigan State University, East Lansing, Michigan 48824, USA*
[3]*National Superconducting Cyclotron Laboratory, Michigan State University, East Lansing, Michigan 48824, USA*
(Received 2 February 2006; published 20 April 2006)

Results from the study of the β decays of ^{40,42}S and ^{43}Cl, produced in the fragmentation of a 70-MeV/nucleon ^{48}Ca beam, are presented. The half-lives for ^{42}S and ^{43}Cl have been measured to be 1.03 ± 0.03 s and 3.13 ± 0.09 s, respectively. On the basis of γ-ray singles and $\gamma\gamma$ coincidence data, decay schemes for each of these decays have been established. Only subtle changes in low-energy nuclear structure, including switching of the order of the 2^- and 3^- states in the odd-odd Cl isotopes, were observed when passing the midpoint of the $\nu f_{7/2}$ subshell. These results agree well with previous shell-model calculations using restricted model spaces suggesting that deformation and shell-breaking effects in the midshell region are small. However, excitations across the $N = 20$ shell gap are important to explain the low-lying positive parity states.

DOI: 10.1103/PhysRevC.73.044318 PACS number(s): 21.10.−k, 21.60.Cs, 23.40.−s, 27.40.+z

I. INTRODUCTION

A major question in nuclear structure physics is whether the magic numbers that appear to hold near stability remain as the drip lines are approached [1]. Nuclei in the proton *sd* shell between the $N = 20$ and 28 shell closures (i.e., the $\nu f_{7/2}$ subshell) have been of interest to this question because of the observation of regions of deformation near the singly magic nuclei ^{32}Mg and ^{44}S. The observed structure in this region depends strongly on the filling of both the proton and neutron orbitals, how their relative energies change as one moves away from stability, and the effects of deformation. To properly understand these effects requires knowledge of nuclear structure as it varies across the full $\nu f_{7/2}$ subshell. Three recent experiments have shed additional light on this subject. A measurement of nuclear masses by Sarazin *et al*. indicates that prolate deformed ground states associated with shape coexistence occur for the heavier Cl, S, and P isotopes [2]. This agrees with the half-life measurements near $N = 28$ by Grévy *et al*. where a theoretical interpretation of the results for the Si isotopes requires prolate or oblate deformation with $|\epsilon_2| \geqslant 0.3$ [3]. However, evidence from a two-proton knockout reaction on ^{44}S suggests that for ^{42}Si the $Z = 14$ subshell closure and $N = 28$ shell closure are well developed and deformation is not present in contradiction to most theoretical calculations [4]. The use of β decay to study excited states in these nuclides provides additional insight to quantify how nuclear structure varies in this region. The results presented here are based on a systematic study of the β decays of neutron-rich P, S, and Cl nuclides.

Nuclei in this region are very favorable for studies using β decay for two basic reasons. First, the large Q-value window means a large number of excited states are available to be populated. Second, the differences in ground-state spins and parities between the parent and daughter limits the possibility for direct feeding to the ground state. This arises from the fact that the protons are filling the $1s_{1/2}$ or $0d_{3/2}$ subshells, whereas the neutrons are filling the $0f_{7/2}$ subshell. For the odd-odd Cl nuclei this means a negative-parity ground state with $J \geqslant 2$ for which direct feeding will not compete with the allowed Gamow-Teller β decay from the S parents to excited 1^+ states. Assuming a first forbidden unique decay this puts an upper limit of less than 0.1% for direct feeding to the ground state. In addition, because positive-parity states will require promoting a proton or a neutron across the shell gap, these intruder states are expected to be at a relatively higher energy with negative-parity states at lower energies. The negative-parity states will be fed by parity-changing $E1$ transitions as the spin increases in reaching the ground state. For the odd-A nuclei, direct decays to the ground state are also expected to be prohibited if a simple single-particle picture holds. For ^{43}Cl, the expected $3/2^+$ ground state will feed either positive-parity $(1/2^+, 3/2^+, 5/2^+)$ or negative-parity $(1/2^-, 3/2^-, 5/2^-)$ states by allowed or first forbidden β decays.

Very little information was known about the β decay of these nuclides prior to this study. Dufour *et al*. measured a half-life for ^{40}S of 8.8 ± 2.2 s and observed four γ rays associated with its decay [5]. Sorlin *et al*. measured a half-life for ^{42}S of 0.56 ± 0.06 s, but no γ rays were observed [6]. For ^{43}Cl, Vosicki *et al*. and Huck *et al*. measured similar half-lives (3.3 ± 0.2 s and 3.4 ± 0.3 s, respectively), whereas Huck *et al*. also produced a preliminary level scheme for ^{43}Ar [7,8].

Slightly more information is known about the low-energy structure of the daughter nuclides. Excited states in ^{40}Cl were first identified in (^{7}Li,^{7}Be) and (^{11}Be,^{11}C) charge-exchange reactions on ^{40}Ar [9]. Two additional experiments using the ^{9}Be(^{36}S,αp)^{40}Cl reaction [10,11] have resulted in identification of states with spins from 1 to 8, most likely all being of negative parity. Of these, only a state at 211 keV could be positively associated with a γ ray observed

*Electronic address: j.a.winger@msstate.edu; on sabbatical with the University Radioactive Ion Beam (UNIRIB) Consortium, the Joint Institute for Heavy Ion Research, the Center for Excellence in Radioactive Ion Beam Studies for Stewardship Science.

in the β-decay experiment [5,11]. Hence, the β decay is populating a different set of lower-spin states than those populated by the heavy-ion reaction. For ^{43}Ar, four excited states were observed by Jelley *et al*. using the ^{48}Ca(α,^{9}Be)^{43}Ar reaction [12], whereas Maréchal *et al*. used inelastic proton scattering with a radioactive ^{43}Ar beam to identify a separate state [13]. Only the state at 1.74 ± 0.05 MeV has a possible corresponding state to those previously observed in β decay [8].

Results presented here are based on data obtained during an experiment studying the decay of ^{40}P [14]. In the experiment it was necessary to isolate and assign all γ rays not associated with ^{40}P decay. This included the decay of the daughter nuclide ^{40}S for which no detailed study had been performed. By making small adjustments to the A1200, as discussed below, nearly pure beams of the two contaminant nuclides (^{42}S and ^{43}Cl) were obtained. This article presents final results from the analysis of the contaminants to the ^{40}P experiment. Preliminary results from this work have been previously published [15].

II. EXPERIMENTAL PROCEDURE

Sources of ^{40}P, ^{42}S, and ^{43}Cl were produced via fragmentation of a 70-MeV/nucleon ^{48}Ca beam in a 254 mg/cm^2 Be target using the A1200 fragment separator of the National Superconducting Cyclotron Laboratory at Michigan State University [16]. The fragments were identified using standard energy loss versus time-of-flight techniques. For the decay of ^{40}P, the A1200 rigidity was scanned and found to provide peak production of the ^{40}P fragments at $B\rho = 2.9073$ Tm. A 3% momentum slit at the first intermediate image of the A1200 was used to make the initial selection of fragment ions. Further separation of the fragment ions was obtained by use of a thin achromatic wedge (pressed plastic with a thickness of $\sim$200 mg/cm^2) placed at the second intermediate image of the A1200. After passing through the wedge, the ^{40}P ions were centered at the focal plane of the A1200 by tuning the second half of the device to $B\rho = 2.5316$ Tm. For this setting, 45% of the beam was ^{40}P with the major contaminants being ^{43}Cl (43%) and ^{42}S (8%). By reducing the rigidity of only the second half of the A1200 by 0.4% ($B\rho = 2.5215$ Tm), the ^{42}S ions were centered in the focal plane and resulted in a beam that was 93% pure. In the same way, the ^{43}Cl ions were centered at the focal plane by increasing the rigidity by 0.1% ($B\rho = 2.5341$ Tm) resulting in a 93% pure beam. Figure 1 shows the particle identification plots (energy loss versus time of flight) observed at each of the three settings. Although this method does not provide the highest possible rate for ^{42}S or ^{43}Cl, it does give a beam with a higher purity and a rate sufficient to obtain good statistics in a short time.

For each setting, the beam was transported to the detector end station [14] located approximately 40 m downstream from the A1200. Identification of the ions transported to this location was obtained using a 500-μm Si PIN diode near the beam-line exit for energy loss determination with the time-of-flight measurement being made relative to a thin plastic detector placed just downstream from the A1200

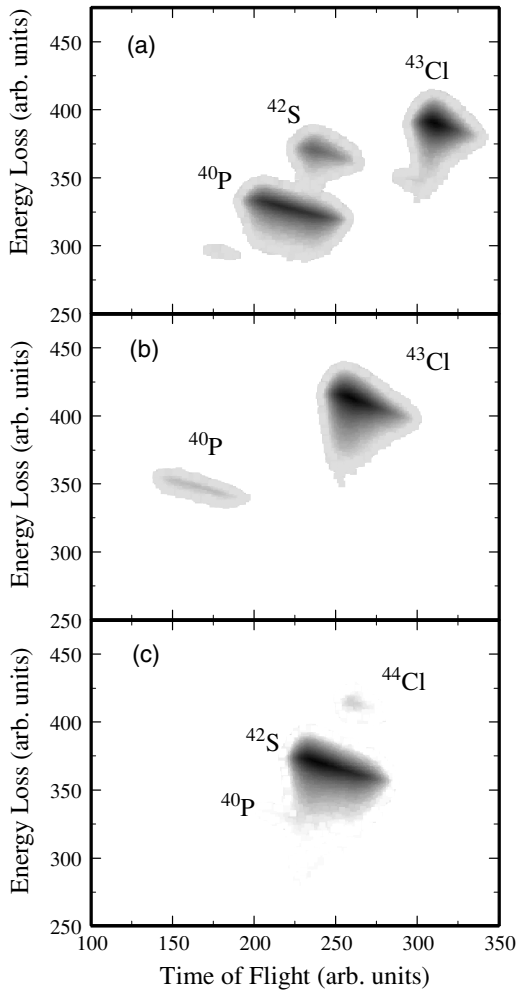

FIG. 1. Particle identification (PID) plots (energy loss in Si PIN diode versus time of flight) at the three settings of the A1200. A 2% lower-level cutoff has been applied. (a) PID plot with the A1200 tuned for maximum production of ^{40}P. (b) PID plot with ^{43}Cl centered at focal plane. (c) PID plot with ^{42}S centered at the focal plane.

exit. These detectors allowed precise determination of the components of the beam. The ions exited the beam line through a 5-mil Kapton window, which was followed by a 16-mil layer of Al foil for slowing the ions, and were then imbedded into 17-mil Al targets attached to a rotatable wheel that was oriented at 45° relative to the beam direction. The wheel allowed setting various beam-on/beam-off timing cycles to study different beam components. The decays of the implanted ions were observed using three detectors: a 1-mm-thick plastic scintillator β detector located directly downstream of the target, an 80% Ge detector directly behind the β detector and 1.8 cm from the target, and a 120% Ge detector oriented at 90° relative to the beam direction and 4.1 cm from the center of the target. The full-width-at-half-maximum (FWHM) energy resolution of the two Ge detectors was 2.5 and 2.9 at 1332 keV, respectively. The measured absolute photopeak efficiencies range from 8.2 and 5.8% at 122 keV to 2.7 and 2.2% at 1332 keV, with extrapolated values of 1.1 and 0.77% at

4 MeV [14]. Timing signals from the three detectors were used to set hardware timing gates. Data from the detectors were only collected when two of the detectors were in coincidence based on these timing gates. Further refinement using software gates during off-line analysis provided information on $\beta\gamma$ and $\gamma\gamma$ coincidences. In addition, the time of each event relative to the beginning of a decay cycle was recorded. The clock for this measurement was reset at the end of each cycle and not restarted until the start of the next decay cycle so that during the growth phase of the timing cycle events did not have a time recorded. Additional details on the detection system can be found in Ref. [14].

For each A1200 setting, β-gated γ-ray spectra for both Ge detectors were obtained. These spectra were analyzed separately to obtain γ-ray energies and relative intensities. Final energies and intensities were obtained using weighted averages between the runs for each detector and then for the two detectors. For the intensities, corrections for coincidence summing based on the proposed level schemes were made. In the ^{42}S and ^{43}Cl measurements, γ rays down to relative intensities of $<0.5\%$ were measured, whereas for ^{40}S the limit was $\sim 1.0\%$. Background-subtracted coincidence γ-ray spectra were obtained and analyzed, providing the information used to develop the decay schemes shown in the following sections. In the proposed decay schemes, levels firmly established by coincidence information and crossover transitions are indicated by solid lines. Other proposed levels are dashed if the order of a cascade is uncertain or if the level is established by a single transition. Any γ rays linking dashed levels or not supported by coincidences are also dashed because their placement is uncertain.

For each mass, only one member of the mass chain was separated in this experiment, making it possible to directly measure the ground state or unobserved feeding by using a saturation spectrum in which a comparison of the parent decay to known decays in their daughters or granddaughters is made. (See Ref. [14] for details on this method.) This allowed determination of absolute level feedings that are presented for all levels in the decay schemes unless the intensity balance indicated no feeding to that level. The reported feedings should be viewed as upper limits because feeding from higher-lying unobserved states would reduce their values. This technique was not possible for the case of ^{42}S as will be discussed below. Based on the apparent absolute feedings to the observed levels, lower limits for the log(ft) values were determined. In this analysis, the newly measured half-lives for ^{42}S and ^{43}Cl were used along with Q_β values taken from the 2003 Mass Tables [17]. Although the log(ft) values do not firmly establish the spins and parities of the states, they do provide guidelines on the range of values possible.

The following sections contain discussions for each decay and conclusions that can be drawn from these results. To simplify the presentation, all information on γ-ray energies and intensities, level energies and apparent feedings, and estimated log(ft) values will be given only in the decay scheme figure. A table of coincidence relationships will be given for reference. For each decay, the relative intensities are based on 100 for the most intense transition and the absolute normalization value will be given in the text.

III. DECAY OF ^{40}S

The decay of ^{40}S was observed following the decay of the ^{40}P component of the beam. The data used for the ^{40}S decay were obtained during two separate saturation measurements (of 41 and 36 min duration, respectively) as well as a timing cycle of 20 s beam on (90 min). During these measurements a total of 3.4×10^5 ^{40}P ions were implanted into the wheel at an average rate of $\sim$35 ions/s. Because of the timing cycles used in this measurement it was not possible to measure the half-life. A total of 12 γ rays that deexcited 6 levels in ^{40}Cl were associated with this decay. Coincidence information for the γ rays is provided in Table I, whereas the decay scheme is shown in Fig. 2. The placement of the 431-keV γ ray in parallel to the 211-keV γ ray is evidenced by the coincidence spectra shown in Fig. 3. All the proposed levels are well established by coincidence and energy sum relationships. The strongest γ ray observed is at 211 keV and corresponds to the deexcitation of the first excited state [11]. The 431-, 677-, and 889-keV γ rays were also observed by Dufour *et al.* but were not placed in a level scheme [5]. Balamuth *et al.* also observed the 211-, 431-, and 677-keV γ rays but were only able to place the 211-keV γ ray in the level scheme [11]. All three γ rays were found to be consistent with dipole transitions in Ref. [11].

The absolute intensity normalization was based on the relative intensities of the 1460-, 2622-, 2839-, and 3101-keV γ rays associated with the β decay of ^{40}Cl observed in the saturation spectra. Although the 1460-keV γ ray is present in the background, the β gating reduced the background component to negligible levels. This established the absolute normalization factor to be 0.52 ± 0.03 for the ^{40}S decay. Using this value the level feedings presented in Fig. 2 were obtained. This intensity balance analysis indicates that there is no significant feeding to the levels at 211 and 431 keV, whereas the sum of feeding to the ground state indicates a missing feeding of $3 \pm 9\%$. This latter result is consistent within the measurement uncertainty with the expectation that there is no feeding to the ground state. The assignment of 2^- for the ground state of ^{40}Cl was based on low log(ft) values for decay to known negative parity states in ^{40}Ar [18]. This

TABLE I. Coincidence relationships for γ rays assigned to ^{40}S decay.

E_γ(keV)	Coincident γ rays (keV)[a]
211.59	(403), 677, (705), 1013, 1081, 1786
403.70	677, 889, 1013
431.57	457, 1874
457.4	431
677.41	211
705.20	(1081),(1292)
889.04	403, 1013
1013.57	211, 403, (889), 1081, 1292
1081.33	211, (705), 1013
1292.87	(705), 1013
1786.6	211
1874.41	431

[a]Weaker coincidence relationships are indicated in parentheses.

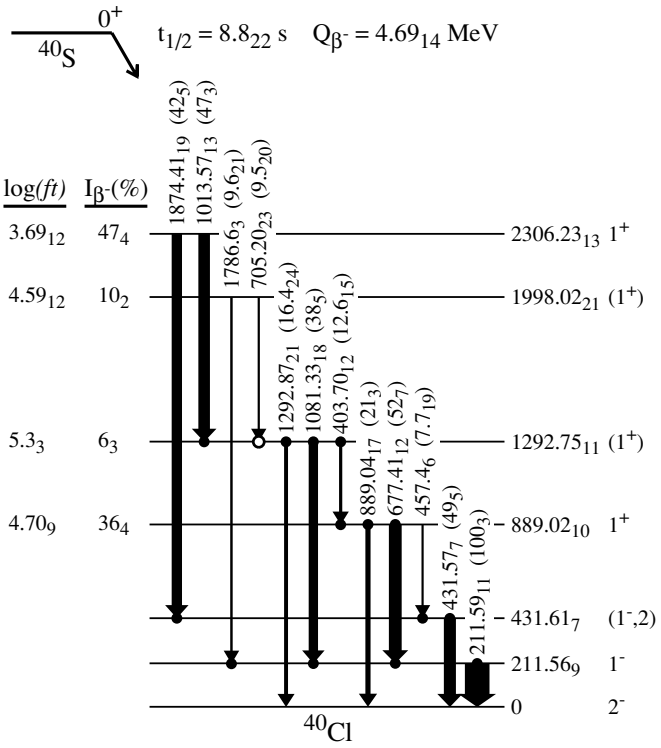

FIG. 2. Decay scheme for ^{40}S into states of ^{40}Cl. The half-life comes from Ref. [5], whereas the Q_β value comes from Ref. [17]. Closed circles indicate firm coincidence relationships, whereas open circles indicate weak coincidence information. See text for discussion of spin and parity assignments.

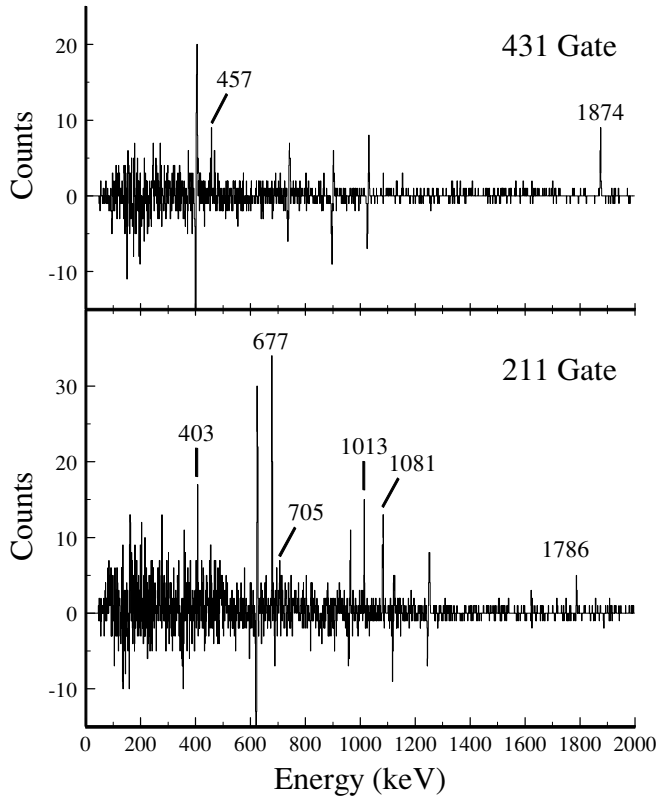

FIG. 3. Background-subtracted coincidence spectra gated on the 211- and 431-keV γ rays associated with the decay of ^{40}S. γ rays observed in coincidence are indicated by their energy in keV. Several large backscatter peaks are also observed.

assignment is consistent with the results presented here and the expectations from a simple shell-model picture. Shell-model calculations [19–21] all predict the ground state to be 2^- with a β decay feeding of $<0.5\%$.

The decay scheme observed for ^{40}S follows the general expectations discussed previously. The states at 889 and 2306 keV are strongly fed ($I_\beta > 30\%$) with low log(ft) values indicative of allowed β decay. The levels at 1292 and 1998 keV also have apparent nonzero feeding, but the large uncertainties and the possibility of feeding from unobserved states makes a definite assignment impossible. The 1^+ levels at 889 and 1292 keV both have ground-state transitions (presumedly $E1$) that are not observed for the two higher lying 1^+ states. The nonobservation of these transitions places their relative intensity at $<2\%$.

Of the levels observed, only the state at 211 keV was previously identified [11]. (see Fig. 4). All of the higher spin ($J \geqslant 2$) states observed in Ref. [11] are not fed in the β decay or by the cascades down to the ground state. This can be understood from the fact that $\Delta J = 1$ transitions should dominate the decay so that states with spins of $J \geqslant 3$ are unlikely. The 211-keV level appears to be the first excited state in ^{40}Cl based both on the results presented here and the heavy-ion reactions [10,11]. In these earlier measurements, the 211-keV level was only weakly populated. The three shell-model calculations all predict a low-lying 1^- state [19–21], indicating a multipolarity for the 211-keV transition of $M1 + E2$. This appears consistent with the observed deexcitation of the 889-keV level that has presumed $E1$ transitions to both the ground state and the first excited state.

It is hard to establish a firm assignment for the state at 431 keV. It has strong transitions to both the 2^- ground state and the 1^+ state at 2306 keV. Limiting these transitions to either $E1$ or $M1 + E2$ restricts the spin to be 1 or 2. The lack of direct β feeding further precludes a 1^+ assignment. No transition between this state and the 211-keV state ($E_\gamma = 220$ keV) was observed in either singles or coincidence data. This puts an upper limit on such a transition of $<1\%$. This nonobservation indicates a significant difference in the structure of these two states. The shell-model calculations predict an additional low-lying 2^- state [19,20], as well as a 2^+ state that is the lowest-lying positive-parity state (Fig. 4) [19]. It is certainly possible that either of these states could be the the one observed. However, the 2^- state should be observed in the heavy-ion reactions. A state at 367 keV has been proposed for this state in Ref. [11] and the 431-keV transition was observed but not placed. Assignment as a 2^+ state is slightly favored based on the combination of experimental and theoretical evidence.

A direct comparison to the shell-model calculation of Warburton and Becker [19] gives some additional insight into this decay. The calculation was preformed using the Warburton-Becker-Millener-Brown (WBMB) interaction

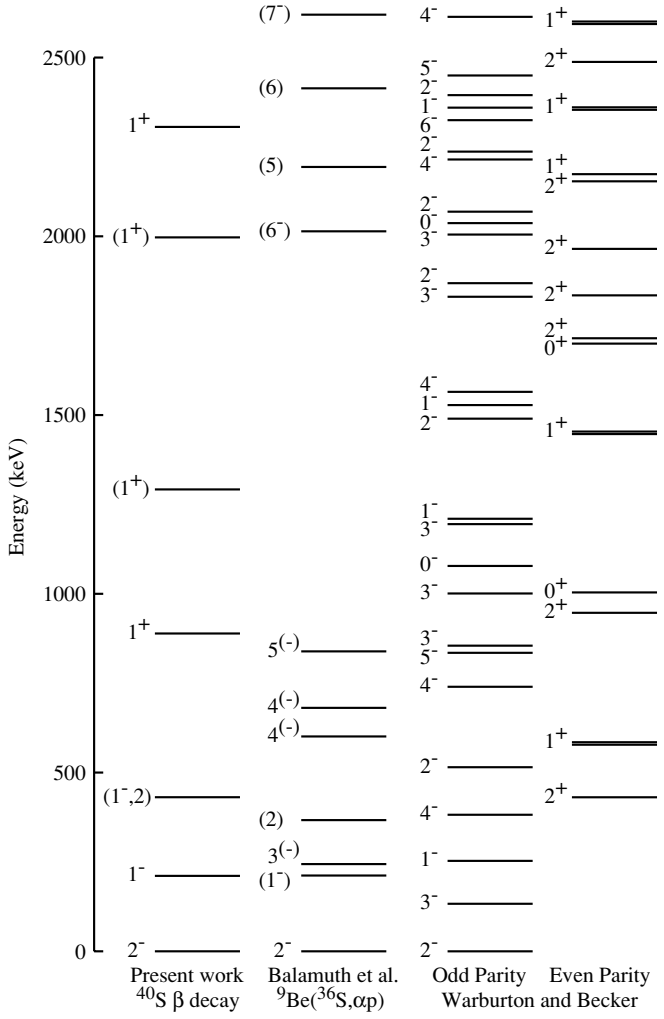

FIG. 4. Comparison of the level scheme for ^{40}Cl from this experiment to the experimental results of Balamuth *et al.* [11] and the theoretical calculations of Warburton and Becker [19]. The even-parity states from the calculation of Warburton and Becker have been shifted under the assumption that the 2_1^+ state is at 431 keV. The 1^+ states estimated to reach the detection limit of this experiment are indicated by thicker lines.

within an *nfp* model space. The odd-parity states were obtained with the full $3fp$ model space, whereas the positive-parity states come from a severely truncated $4fp$ model space using only 24 partitions. In Fig. 4, all negative-parity states are shown, whereas only the $J \leqslant 2$ positive parity states are shown. In the calculation, the position of the positive-parity states relative to the negative-parity states could not be determined. By assigning the 431-keV level as the 2_1^+ state, as shown in Fig. 4, we can consider the relative placement of the 1^+ states predicted to be fed in the β decay.

For the Gamow-Teller operator, Warburton and Becker used the effective *sd* shell operators of Brown and Wildenthal [22,23] along with a modified form of the fundamental results from Towner [24]. This operator was used to calculate the B(GT) values for all energetically accessible 1^+ states. Of these states, 15 were predicted to receive >99% of the Gamow-Teller

TABLE II. Estimated β-decay feedings and log(ft) values based on the theoretical results of Warburton and Becker [19].

State	E_γ(keV)	Iβ(%)	log(ft)
1_1^+	585	15	5.55
1_2^+	1454	28	4.82
1_4^+	2361	43	4.01
1_5^+	2601	4	4.80
1_6^+	2739	2	4.99
1_7^+	2874	2	4.86
1_{11}^+	3303	3	4.30

β decay strength and were listed in Ref. [19]. The estimated log(ft) values for these states range from 4.01 to 6.72. This can be contrasted to the calculated first-forbidden decay strength that was found to be <1% of the total feeding with log(ft) > 6.34 and $I_\beta < 0.34\%$ for any negative-parity state, providing support to the assumption that only 1^+ states should have been observed to be fed. The B(GT) values obtained in the calculation depend strongly on the composition of the states connected by the Gamow-Teller transition. Unfortunately, Warburton and Becker listed only the composition of two states of interest, the 0_1^+ state in ^{40}S and the 1_1^+ state in ^{40}Cl (see Table II in Ref. [19]). For these states, only the $s_{1/2}$, $d_{3/2}$, $f_{7/2}$, and $p_{3/2}$ subshells make significant contributions to the wave function (i.e., the $d_{5/2}$ subshell and lower remain filled). Because excitation into the $\pi p_{3/2}$ subshell is unlikely, only the other three subshells are involved in the decay. The ^{40}S ground state is primarily composed of terms with $\nu f_{7/2}^4$ coupled to $\pi d_{3/2}^{-2}$ or $\pi s_{1/2}^{-1} d_{3/2}^{-3}$. The composition of the ^{40}Cl 1_1^+ state is dominated by terms involving excitation of a neutron across the $N = 20$ shell gap to produce hole states in the $\nu d_{3/2}$ and $\nu s_{1/2}$ subshells. The β decay then involves the $\nu d_{3/2} \rightarrow \pi d_{3/2}$ and $\nu s_{1/2} \rightarrow \pi s_{1/2}$ transitions to produce the hole states.

Using the B(GT) values from Ref. [19] and the known Q value [17], we estimated the β-decay feeding to the 15 1^+ states. In this calculation, a theoretical half-life of 18.6 s was needed to obtain a total for the allowed β-decay feeding of 99%. Of the states, seven would reach the detection level of this experiment. Information on these states is given in Table II and have been indicated by thicker lines in Fig. 4. The strongest fed state [1_4^+ with $I_\beta \sim 43\%$ and $\log(ft) = 4.01$] is predicted to lie 1.9 MeV above the 2_1^+ state (2361 keV in Fig. 4), which agrees well with the observed state at 2306 keV. The 1_1^+ and 1_2^+ states have log(ft) values similar to the 1292- and 889-keV states, respectively. The difference in observed feeding is primarily because of the difference in energy between the observed and theoretical states. The state observed at 1998 keV could be one of the other four 1^+ states from the calculation, with the lower energy giving a higher feeding. The overall agreement between experiment and theory is quite good even with the truncated model space for the even parity states.

IV. DECAY OF ^{42}S

The data for ^{42}S decay was obtained using beam-on/beam-off timing cycles of 15 s/15 s (81 min) and 3 s/6 s (150 min) as

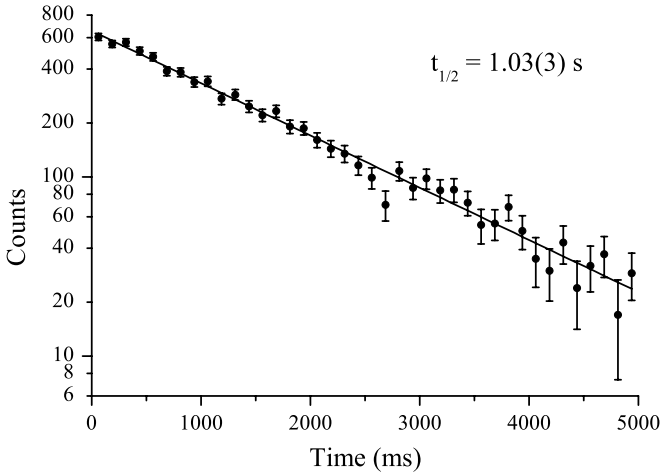

FIG. 5. Half-life curve for ^{42}S β decay using gates set on the 118-, 470-, and 723-keV γ rays with background gates subtracted.

well as in saturation (103 min). During these measurements, a total of 1.6×10^6 ^{42}S ions were implanted into the wheel at an average rate of $\sim$130 ions/s. The strongest γ rays associated with this decay have energies of 118, 470, 723, and 1281 keV. The half-life was determined using gates set on the first three of these γ rays with adjacent background gates subtracted. The 1281-keV γ ray was not used because of contamination from an adjacent γ ray (1283 keV) from ^{42}Cl decay. The time spectrum obtained is shown in Fig. 5. This spectrum was fitted with a single decaying exponential yielding a half-life of 1.03 ± 0.03 s. This value differs by almost a factor of 2 with the previously reported value of 0.56 ± 0.06 s by Sorlin *et al*. [6]. However, the earlier result was based on a small number ($\sim$350) of correlated fragment-β events. The use of γ-ray gated time spectra in this study assures a more accurate determination of the half-life.

A total of 41 γ rays that deexcited 17 levels in ^{42}Cl were associated with this decay. Coincidence relationships for the γ rays are provided in Table III, whereas the decay scheme is shown in Fig. 6. The lower-level cutoff for relative intensities of γ rays observed in this measurement was $<$0.5% up to an energy of 4 MeV. All γ rays with relative intensities greater than 1% have been either assigned as depopulating excited states in ^{42}Cl or associated with another decay based on the available coincidence data and energy-sum relationships.

The majority of the levels shown in Fig. 6 are firmly established by coincidence and energy-sum relationships. The levels at 1576, 1684, 1834, and 2221 keV are intermediate levels in a two-γ-ray cascade linking established levels. Reversing the order of the cascades would yield levels at 1571, 439, 877, and 2358 keV, respectively. For the 1834-keV level the ordering of the cascade is based on the statistically significant higher intensity of the 1245-keV γ ray. The choice of a level at 1684 keV over 439 keV is based on the assumption that a lower-lying level would probably have feeding from other states. None of these levels is expected to receive significant β-decay feeding. The level at 2403 keV is based on a single transition that is suggested by the coincidence relations and would receive direct feeding.

TABLE III. Coincidence relationships for γ rays assigned to ^{42}S decay.

E_γ(keV)	Coincident γ rays (keV)[a]
118.25	(252), 425, 470, (521), 678, 685, 723, 1121, 1149, 1245, 1281, 1318, 1453, 1458, 1592, 2004, 2187, 2440, 2911
160.60	1318, 1550
202.42	118, 521, 639
252.6	118, (470), (1281)
288.49	(470)
425.61	118, 723, 841
439.09	1684
470.78	118, (288), 547, 678, 796, 1121, 1245, 1318, 1534, (1814), 2440
521.26	118, 202, 470, 1071, 1281
588.78	678, 1534
638.9	202, (1281), (1318)
670.55	808, 1550
678.43	(118), 470, 588
685.1	118, 907, 1318
723.72	118, 425, (868), 1281, 1399, 2187
737.8	118, (470)
796.80	470
808.55	118, 670, (1550)
841.95	425, 1281
868.94	118, (723), 1318
907.5	118, 685, 1318
1025.9	(685), (1318)
1071.6	118, 521, (1318)
1121.97	118, 470, 1318
1149.42	118
1245.93	118, (288), 470
1281.44	118, 723, 841
1318.88	118, 160, 470, (521), (639), 685, (868), (1025), (1071), 1121, 1550, (1592)
1399.1	(118), 723
1453.2	118, 1458
1458.53	118, 1453
1534.26	118, 470, 588
1550.52	160, 670, (808), 1318
1592.55	118, (1318)
1652.4	(118)
1684.1	439
1814.2	(470)
2004.93	118
2187.2	118, 723
2440.60	118, 470
2911.7	118

[a]Weaker coincidence relationships are indicated in parentheses.

The absolute intensity normalization could not be made for this decay based on consideration of the known γ rays from the decays of the daughter and granddaughter for two reasons. First, the absolute normalization for the decay of ^{42}Cl is not known even though some information on the decay is known [8]. Second, the long half-life of ^{42}Ar made it impractical to achieve saturation for its decay. Hence, a different method was used in this case. From the decay of ^{40}S we find

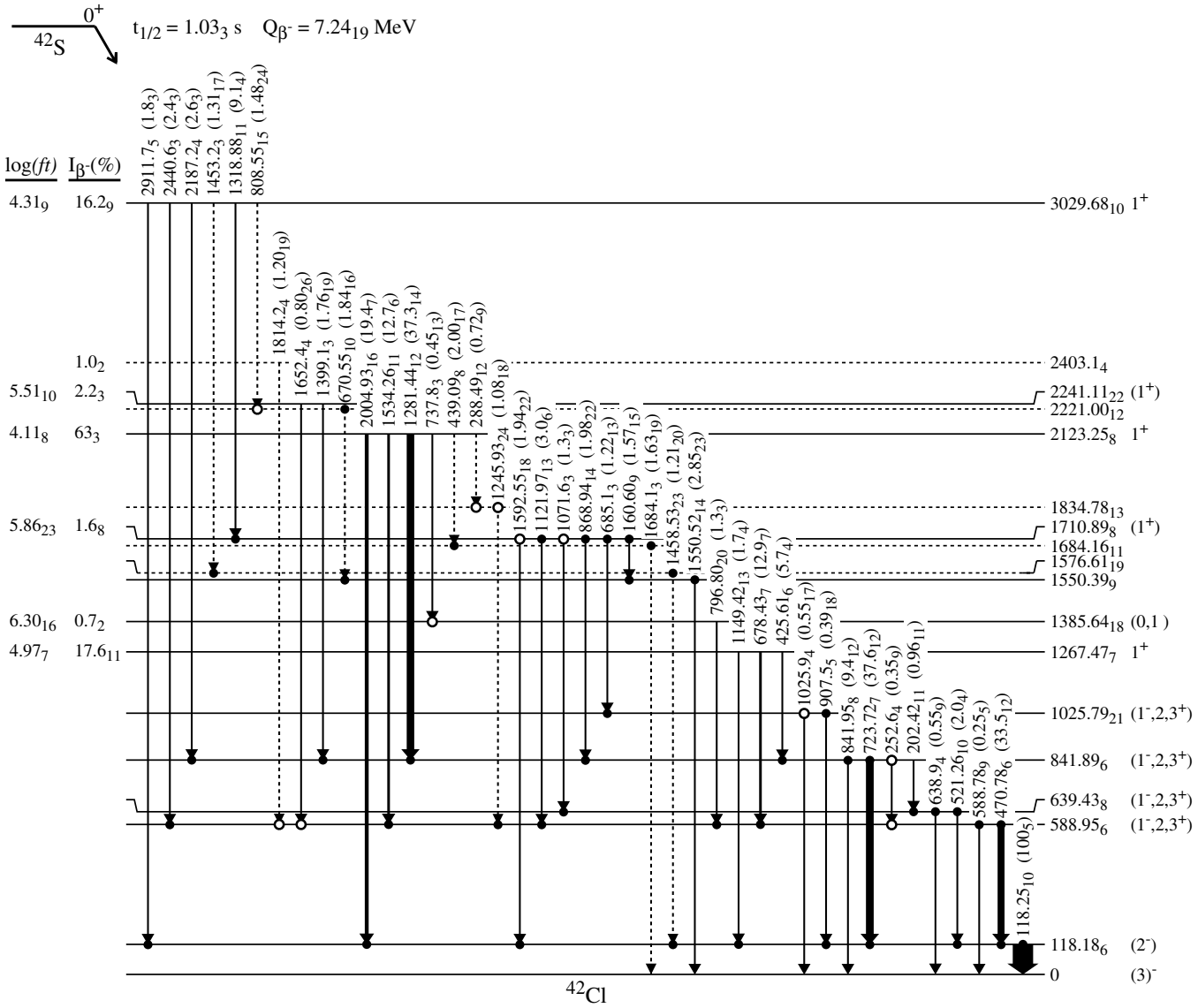

FIG. 6. Decay scheme for ^{42}S into states of ^{42}Cl. The Q_β value comes from Ref. [17]. Closed circles indicate firm coincidence relationships, whereas open circles indicate weak coincidence information. See text for discussion of spin and parity assignments.

that the feeding to the ground state is negligible. For reasons that will be argued later, there is a strong indication that the ground state of ^{42}Cl is 3^-, which would completely preclude a direct decay. Therefore, it is reasonable to assume within the limits of this measurement that there is no direct ground-state feeding observed. A small energy window exists for β-delayed neutron emission. A γ ray at 167 keV with a relative intensity of $0.7 \pm 0.2\%$, which may correspond to to a known transition in the decay of ^{41}Cl, was observed in the saturation spectrum for one of the Ge detectors. However, there is no evidence in the data for other γ rays associated with this decay, which should have the same or a greater intensity. The intensity of the 167-keV γ ray sets $P_n < 1\%$. Hence, we have used only the sum of all the γ-ray intensity feeding the ground state to establish the normalization. This results in an absolute normalization factor of 0.87 ± 0.04 for the ^{42}S decay. This normalization leads to a total deduced β feeding of $100 \pm 6\%$ and is used to determine the apparent level feedings and log(ft) values presented in Fig. 6.

The levels at 1267, 2123, and 3029 keV receive >96% of the feeding and are firmly established as 1^+ states. The levels at 1710 and 2241 keV have log(ft) values between 5 and 6, which suggests they are also 1^+ states. The level at 1385 keV has a log(ft) value greater than 6, indicating either an allowed or a first forbidden β decay. The intensity balance analysis indicates that there is no significant feeding to any of the levels below 1.1 MeV. These states could then either have negative parity or be positive-parity states with $J \neq 1$.

No prior information is known about excited states in ^{42}Cl. However, some additional insight into the spin and parity assignments for the states below 1.1 MeV can be inferred by a comparison to the decay of ^{40}S. In terms of the shell-model

structure, the only difference between ^{40}Cl and ^{42}Cl is the addition of two neutrons into the $\nu f_{7/2}$ subshell. The result is two level schemes that are strikingly similar with a number of 1^+ states being directly fed by β decay that deexcite to the ground state through a number of low-lying energy levels. The most striking difference occurs when comparing the ground state and first excited state. In ^{40}S decay, two transitions (211 and 431 keV) with comparable intensities are observed to feed the ground state but for which their originating levels are not connected. In ^{42}S decay only one strong transition to the ground state is observed, at 118 keV, which carries 86% of the intensity. In addition, although two of the 1^+ states in ^{40}Cl have transitions to the ground state there are no direct transitions to the ground state in ^{42}Cl from states directly fed by the ^{42}S β decay. The implication from this is that there is a switching of the order between the low-lying 2^- and 3^- states. Additional support for a 3^- assignment for the ground state comes from analysis of the β decay of ^{42}Cl, which was also observed in this experiment. In this decay, the intensity balance indicates no feeding to the 2_1^+ state in ^{42}Ar, whereas there is nearly equal feeding to the 2_2^+ and 4_1^+ states (4.1 ± 1.0 and $4.5 \pm 2.3\%$, respectively), which yields log(ft) values of 6.74 ± 0.11, and 6.71 ± 0.23, suggesting first forbidden β decay to both states. The experimental results presented in Refs. [8,25] and the shell model calculation in Ref. [26] provide additional support for this assignment. In addition, the trend from systematics in which the 3^- state drops from 755 to 244 keV above the 2^- state in going from ^{38}Cl to ^{40}Cl [11,27] suggests that the two states may switch order.

Spin and parity assignments for the other four low-energy states is more difficult. All have transitions to both the ground state and the first excited state. The levels at 588 and 841 keV are connected by multiple transitions to 1^+ states, whereas the levels at 639 and 1025 keV connect only to the weakly fed 1710-keV level. This makes the 1710-keV level very similar to the 1292-keV state in ^{40}Cl, both of which are tentatively assigned to be 1^+ states but which could be negative parity states. Assuming only $E1$ or $M1 + E2$ transitions would limit these states to $2^\pm$, whereas the possibility for pure $E2$ transitions makes a 1^- or 3^+ assignment feasible.

A comparison of the experimental results to the shell-model calculations of Warburton [26] is presented in Fig. 7. Warburton performed calculations using two model space-interaction combinations. The first calculation used the Hsieh-Mooy-Wildenthal (HMW) interaction within a $(d_{3/2} f_{7/2})^{10}$ model space with up to 5-particle–5-hole excitations with the lowest-lying states being primarily because of neutron excitations. The second calculation used the WBMB interaction within a truncated 5 fp model space [WMB(t)]. The truncation in this case was needed to limit the dimensionality of the model space leading to 4^- states. The WMB(t) interaction predicts nearly degenerate 2^- and 3^- states with a 1^- state at 663 keV and a 2^- state at 1021 keV that could match with two of the observed levels. Although Ref. [26] contains no details on the wave functions of these states, we can gain some additional insight by considering the calculations for ^{40}Cl in Ref. [19]. In this calculation, the 2_1^- and 3_1^- states are dominated by the $\pi d_{3/2}^{-3} \nu f_{7/2}^3$ configuration, 55 and 47%

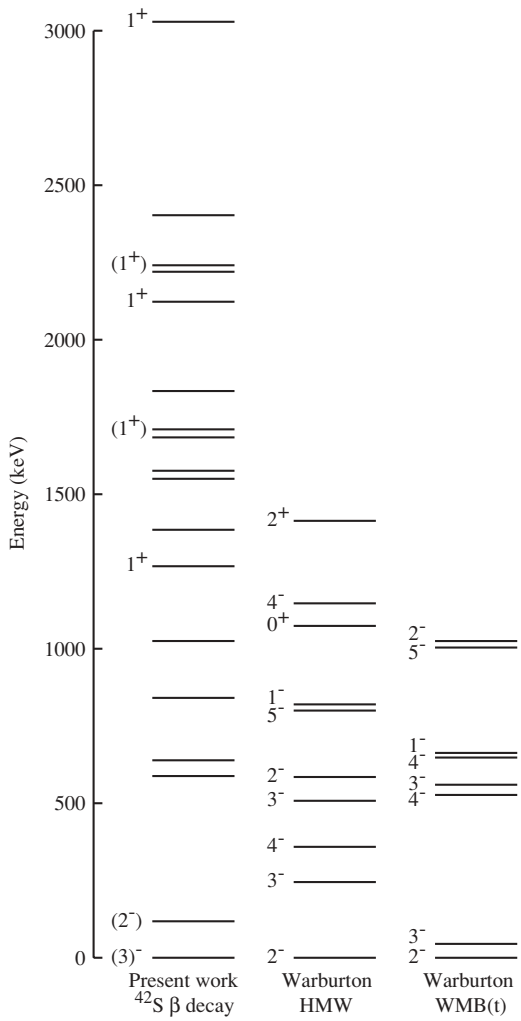

FIG. 7. Comparison of the level scheme for ^{42}Cl from this experiment to the two theoretical calculations of Warburton [26].

respectively, with a significant $\pi s_{1/2}^{-1} d_{3/2}^{-2} \nu f_{7/2}^3$ contribution. The addition of two neutrons should primarily affect the neutron portion of the wave function, which becomes $\nu f_{7/2}^{-3}$, resulting in a modification of the ordering of states and may explain the subtle change in the order of the two states.

The large difference in intensity between the 588- and 470-keV γ rays suggests a change of multipole order with the 588-keV γ ray being an $E2$ transition, whereas the 470-keV γ ray would be $M1 + E2$ with a significant $E2$ component. This suggests that the 588-keV level is the 1^- state predicted by the shell-model calculation [26] and further restricts the 841-keV level to be $2^\pm$ because the 252-, 723-, and 841-keV γ rays appear to have the same multipolarity. The prediction of a 2^+ state at 1.4 MeV with the very truncated HMW interaction indicates that low-lying positive parity states are feasible within the shell model. The conclusion is that we expect two of the states are negative parity $(1^-, 2^-)$ and two are positive parity $(2^+, 3^+)$, but additional experimental information on the multipolarities of the stronger transitions is needed to make more definite assignments possible.

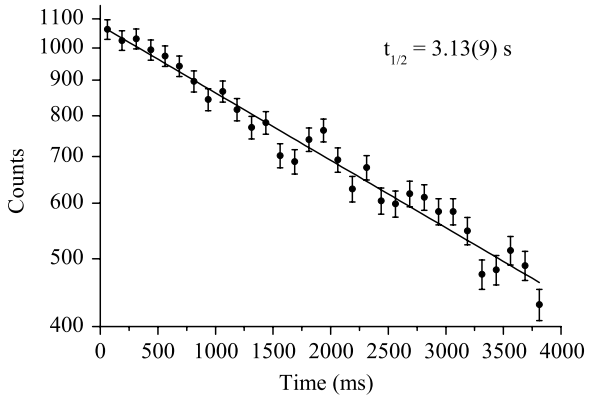

FIG. 8. Half-life curve for ^{43}Cl β decay using gates set on the 761- and 1031-keV γ rays with background gates subtracted.

V. DECAY OF ^{43}CL

The primary data on the decay of ^{43}Cl was obtained using a beam-on/beam-off timing cycle of 4 s/4 s (225 min) with a 93% pure beam. Additional data to establish absolute branching ratios was obtained in the two saturation measurements at the ^{40}P setting. A total of 2.6×10^6 ^{43}Cl ions were implanted into the wheel during the timing cycle measurement at an average rate of $\sim$400 ions/s. This decay is characterized by two intense γ rays (761 and 1031 keV), with no other γ ray having a relative intensity greater than 10%. The half-life of ^{43}Cl was determined using a background-subtracted time spectrum gated by the 761- and 1031-keV γ rays, which is shown in Fig. 8. This time spectrum was fitted with a single decaying exponential yielding a half-life of 3.13 ± 0.09 s. This value is in agreement with the two previous measurements [7,8], but with much better accuracy.

A total of 29 γ rays that deexcited 17 levels in ^{43}Ar were associated with this decay. Coincidence relationships for the γ rays is provided in Table IV, whereas the decay scheme is shown in Fig. 9. The lower-level cutoff for relative intensities for γ rays observed in this measurement was $<0.5\%$ up to an energy of 4 MeV. All γ rays with relative intensities greater than 0.7% have been either assigned as depopulating excited states in ^{43}Ar or associated with another decay based on the available coincidence data and energy-sum relationships. The γ ray at 4247 keV was not directly observed in the experiment because of an energy cutoff at 4.2 MeV. Its energy and intensity are inferred from the observed single and double escape peaks. For the intensity, the ratio of the intensity of the single escape peak to the full-energy peak for a number of high-energy γ rays observed in this and another [28] experiment were used to determine the energy dependency. In addition, the γ ray at 2344 keV was part of an unresolved doublet with a γ ray from ^{43}Ar decay. The intensity was scaled to remove the contaminant. The decay scheme obtained is in good agreement with that given by Huck *et al*. [8], who were able to place 15 γ rays deexciting seven levels.

Of the 17 levels placed in the decay scheme, only 7 are firmly established by coincidence and energy-sum relationships. The level at 1816 is established by a two-γ-ray cascade deexciting the level at 4246 keV with coincidence relationships supporting this placement. The levels at 1944 and 4289 keV are established by a two-γ-ray cascade indicated by coincidences and observation that both γ rays have the proper time behavior for ^{43}Cl. In both cases, the order has the more intense γ ray placed lower. Of the remaining levels, 6 are based on single γ rays but with coincidence relationships supporting the placement. The remaining level (3395 keV) is based on a single γ ray that has the proper time behavior for ^{43}Cl but was not in coincidence with any other γ rays. The only difference with the results of Huck *et al*. is in the placement of a level at 2344 keV that is connected by γ rays to the ground state and 1441-keV level (2344 and 903 keV, respectively). This placement is not supported because there is no evidence in the coincidence spectrum gated on the 679-keV γ ray for a peak at 903 keV, placing an upper limit on its relative intensity of $<0.2\%$.

The absolute intensity normalization was based on the relative intensities of the 738-, 891-, 975-, 1369-, and 2343-keV γ rays associated with the β-decay of ^{43}Ar observed in the saturation spectra. This established the absolute normalization factor to be 0.57 ± 0.08 for the ^{43}Cl decay. Using this value the level feedings and log(ft) values presented in Fig. 9 were obtained. An intensity balance analysis then indicates that

TABLE IV. Coincidence relationships for γ rays assigned to ^{43}Cl decay.

E_γ(keV)	Coincident γ rays (keV)[a]
352.13	679, 761
411.8	619, 761, 1381
619.56	(411), 761, (1008)
679.24	352, (726), 761, 948, (1933), (2108), 2805, 3109
726.58	679, 761, 1031
761.81	352, (411), 619, 679, 948, 1031, (2036), 2390, 2805, (2865) 3109
948.96	679, 761
1008.82	619, (761)
1031.84	726, 761, (2215), 2452
1381.79	411
1441.69	0
1628.1	None
1631.8	(1031)
1758.2	None
1816.5	2430
1933.3	679
1944.96	2344
2036.4	761
2108.0	679
2215.4	1030
2344.0	1944
2390.5	None
2430.0	(761), (1030), 1816
2452.7	(761), (1031)
2805.43	679, 761
2865.7	(761)
3109.3	(679)
3395.8	None
4247.0	None

[a]Weaker coincidence relationships are indicated in parentheses.

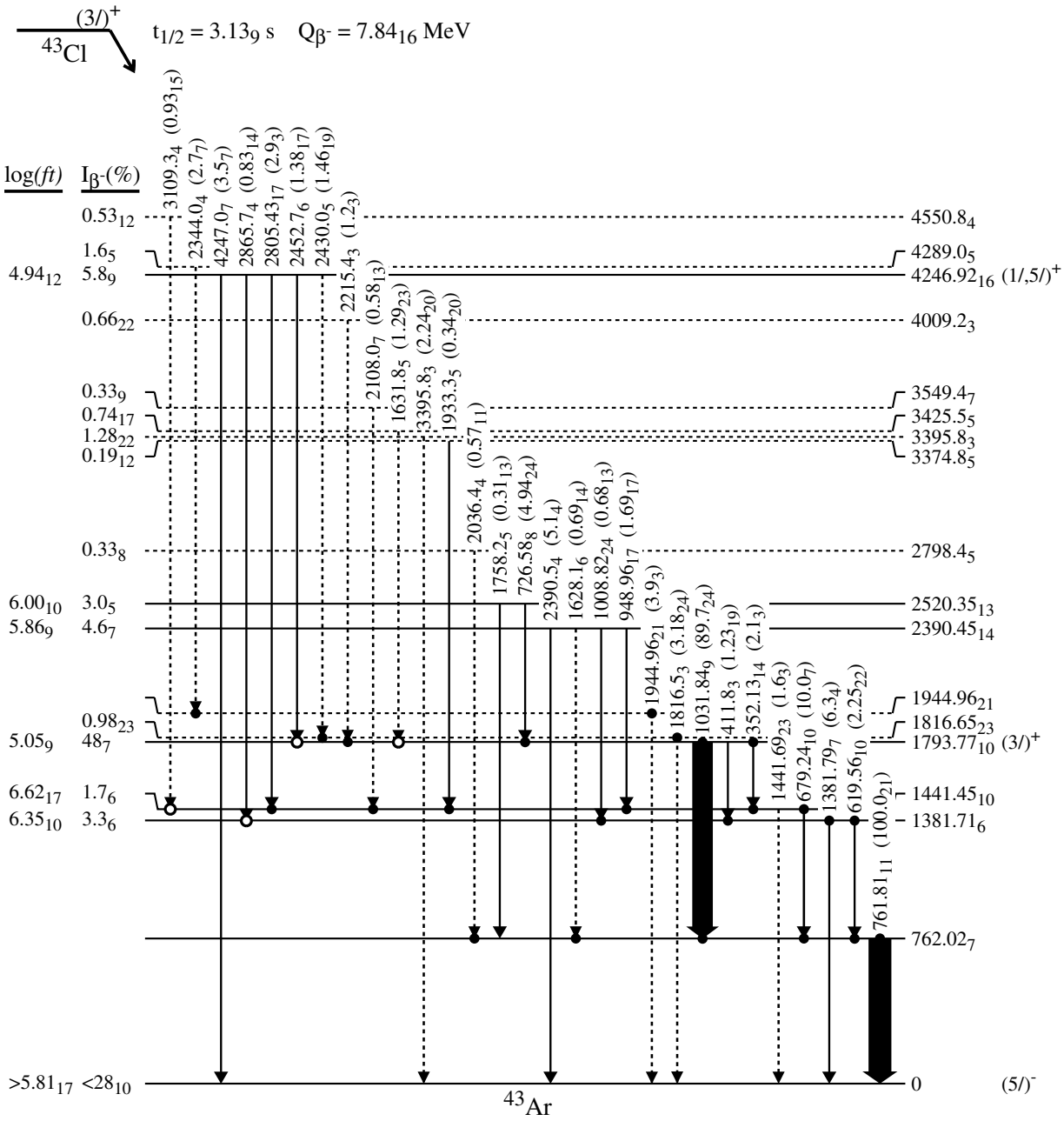

FIG. 9. Decay scheme for ^{43}Cl into states of ^{43}Ar. The Q_β value comes from Ref. [17]. Closed circles indicate firm coincidence relationships, whereas open circles indicate weak coincidence information. See text for discussion of spin and parity assignments.

there is no feeding to the first excited state at 761 keV and the total unidentified feeding is $28 \pm 10\%$. There is no evidence in the data for delayed-neutron branching, therefore, all the unassigned β-decay intensity is attributed to direct feeding of the ^{43}Ar ground state. Such an assumption leads to a log(ft) value of 5.81 ± 0.17, indicating first forbidden decay. We note that this log(ft) value represents a lower limit because unseen γ-ray strength that may directly feed the ^{43}Ar ground state would reduce the apparent β-decay feeding.

The apparent feeding to the ground state by first forbidden β decay from the ground state of ^{43}Cl contradicts the simple assumption that the ground states connected are $\pi d_{3/2}$ and $\nu f_{7/2}$ single-particle states. Although the ground-state spin and parity of ^{43}Cl has not been confirmed experimentally, shell-model studies suggest that the order of the $3/2^+$ and $1/2^+$ states switches order for ^{43}Cl [20,29]. This results from a decrease in the $\pi d_{3/2} - \pi s_{1/2}$ energy difference as the $\nu f_{7/2}$ subshell is filled so that stronger pairing in the $\pi d_{3/2}$ subshell results in a $\pi s_{1/2}$ hole state. The observed prolate deformation [2] would lead to a similar situation. However, both of these situations would further inhibit direct ground-state decay. Evidence from the β decay of ^{43}Ar suggests that the ground state is $5/2^-$ [30]. This assignment is supported by theory as the change from a $\nu f_{7/2}^3$ configuration to a $\nu f_{7/2}^{-3}$

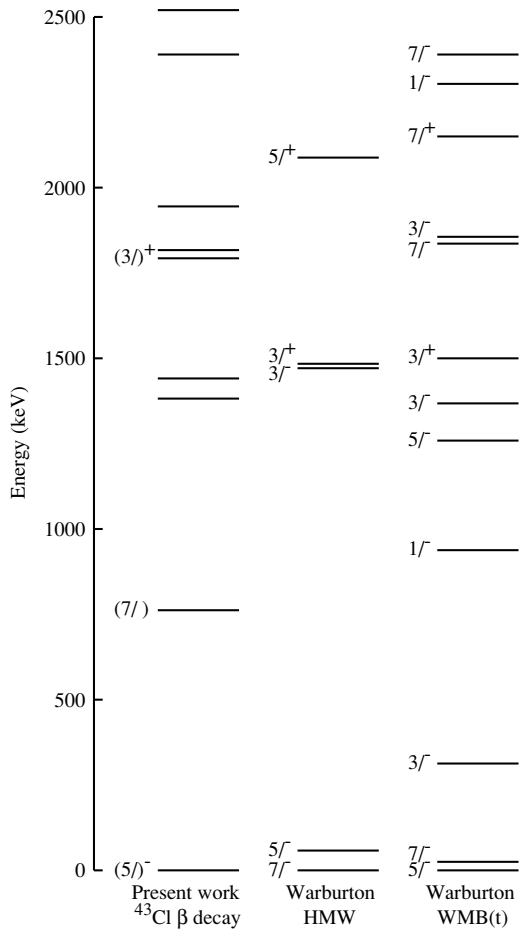

FIG. 10. Comparison of the level scheme for ^{43}Ar from this experiment to the two theoretical calculations of Ref. [26] up to 2.5 MeV. For the theoretical calculations, only states with $J \leqslant 7/2$ are shown.

configuration results in a change in the order of the $7/2^-$ and $5/2^-$ states observed in ^{41}Ar [13,26]. A $5/2^-$ ground state for ^{43}Ar allows the possibility for a first forbidden β decay to occur, but only if the ^{43}Cl ground state is $3/2^+$. Hence, the apparent ground-state feeding leads us to suggest a $3/2^+$ ^{43}Cl ground state. Additional experimental and theoretical studies are needed to clarify the apparent contradiction for this state.

A comparison of the experimental levels to those of Warburton's calculations [26] is presented in Fig. 10. As with ^{42}Cl, calculations were performed using both the HMW and WMB(t) interactions. Both calculations indicate nearly degenerate $5/2^-$ and $7/2^-$ ground and first excited states. Hence, there is substantial experimental and theoretical evidence to indicate that the $5/2^-$ assignment is correct. The lack of observed feeding to the 762-keV level indicates that it has $J \geqslant 7/2$ or that the configuration of the state does not allow feeding by a first forbidden decay. It is not obvious that this is the $7/2^-$ single-particle state, as discussed in the last paragraph of this section.

The apparent β-decay feedings and log(ft) values indicate two states are fed by allowed decays (1793 and 4246 keV) and are therefore positive-parity states with $J \leqslant 5/2$. The dashed level at 4289 keV may also be directly fed by an allowed decay. The remaining levels are more consistent with first forbidden decays although allowed decays cannot be ruled out, especially for the levels at 2390, 2520, 3395, 4009, and 4550 keV. However, the density of positive-parity states is expected to be low, so most of the states will be negative parity. The positive-parity states come from promotion of a neutron across the $N = 20$ shell gap. These $1\hbar\omega$ intruder excitations will primarily have $\nu d_{3/2}^{-1} f_{7/2}^{-2}$, $\nu s_{1/2}^{-1} f_{7/2}^{-2}$, and $\nu d_{5/2}^{-1} f_{7/2}^{-2}$ configurations. Both shell-model calculations (Fig. 10) [26] predict a $3/2^+$ state at $\sim$1.5 MeV in good agreement with the observed level at 1793 keV, whereas one additional positive parity state ($5/2^+$ or $7/2^+$) is predicted between 2.0 and 2.5 MeV. The state at 4246 keV is probably also a one hole state from deeper in the νsd shell.

The exact assignment of J^π for the 762-keV level is not obvious. This level is defined primarily by the 1031–761 cascade. If the assignments of the 1793-keV level and the ground state as $3/2^+$ and $5/2^-$, respectively, are correct then the multipolarities in the cascade must be $M2$(1031)-$M1$(761) for a $7/2^-$ assignment. If this were true then it is expected that an $E1$ transition would compete with the M2 in deexciting the 1793-keV level. A γ ray at 1793 keV is observed but can be shown to be a pure sum peak. Multipolarities in the cascade of $E1$-$M1$ or $M1$-$E1$ also do not fit with the observations because a $J \geqslant 7/2$ state cannot be obtained. Because a low-energy positive-parity state not fed by the decay does not seem likely, it is possible that this level is either the $3/2^-$ or $1/2^-$ state obtained in the shell-model calculation (Fig. 10) [26]. This might be possible if the strength of the β-decay feeding to this level is below the detection limit of this experiment. However, the intensity balance indicates too little intensity deexciting the level. Resolution of this situation will require determination of the multipolarities of the γ rays in the cascade.

VI. CONCLUSIONS

In summary, we have measure the β decays of ^{40,42}S and ^{43}Cl. The half-lives of ^{42}S and ^{43}Cl were measured with greater accuracy. Decay schemes for each nuclide have been produced. For the odd-odd Cl isotopes, the ordering of the low-lying 2^- and 3^- states are observed to switch in passing through the midpoint of the $\nu f_{7/2}$ subshell. In ^{43}Ar, the $5/2^-$ ground-state assignment is given additional experimental support by observation of possible direct ground-state feeding in the decay. However, the structure of the lowest excited state observed in the decay does not fit any simple explanation. There is no indication of dramatic changes in shell structure, with only subtle changes such as the change in order of the 2^- and 3^- states. The good agreement between the present experimental results and the earlier shell-model calculations using truncated model spaces indicates that these nuclides are well behaved in terms of a spherical shell-model approach. The calculations also indicate the importance of neutron excitations across the $N = 20$ shell gap which are needed to explain the low-lying positive parity states.

ACKNOWLEDGMENTS

This work was supported by the U.S. Department of Energy under contract DE-FG02-96ER-41006, by the National Science Foundation under contract PHY-95-28844, and by the UNIRIB consortium under contract DE-AC05-06OR23100 between the U.S. Department of Energy and Oak Ridge Associated Universities.

[1] D. Warner, Nature **430**, 517 (2004).
[2] F. Sarazin, H. Savajols, W. Mittig, F. Nowacki, N. A. Orr, Z. Ren, P. Roussel-Chomaz, G. Auger, D. Baiborodin, A. V. Belozyorov, C. Borcea, E. Caurier, Z. Dlouhý, A. Gillibert, A. S. Lalleman, M. Lewitowicz, S. M. Lukyanov, F. de Oliveira, Y. E. Penionzhkevich, D. Ridikas, H. Sakuraï, O. Tarasov, and A. de Vismes, Phys. Rev. Lett. **84**, 5062 (2000).
[3] S. Grévy, J. C. Angélique, P. Baumann, C. Borcea, A. Buta, G. Canchel, W. N. Catford, S. Courtin, J. M. Daugas, F. de Oliveira, P. Dessagne, Z. Dlouhy, A. Knipper, K. L. Kratz, F. R. Lecolley, J. L. Lecouey, G. Lehrsenneau, M. Lewitowicz, E. Liénard, S. Lukyanov, F. Maréchal, C. Miehé, J. Mrazek, F. Negotia, N. A. Orr, D. Pantelica, Y. Penionzhkevich, J. Péter, B. Pfeiffer, S. Pietri, E. Poirier, O. Sorlin, M. Stanoiu, I. Stefan, C. Stodel, and C. Timis, Phys. Lett. **B594**, 252 (2004).
[4] J. Fridmann, I. Wiedenhöver, A. Gade, L. T. Baby, D. Bazin, B. A. Brown, C. M. Campbell, J. M. Cook, P. D. Cottle, E. Diffenderfer, D.-C. Dinca, T. Glasmacher, P. G. Hansen, K. W. Kemper, J. L. Lecouey, W. F. Mueller, H. Olliver, E. Rodriguez-Vieitez, J. R. Terry, J. A. Tostevin, and K. Yoneda, Nature **435**, 922 (2005).
[5] J. P. Dufour, R. Del Moral, A. Fleury, F. Hubert, D. Jean, M. S. Pravikoff, H. Delagrange, H. Geissel, and K.-H. Schmidt, Z. Phys. A **324**, 487 (1986).
[6] O. Sorlin, D. Guillemaud-Mueller, R. Anne, L. Axelsson, D. Bazin, W. Böhmer, V. Borrel, Y. Jading, H. Keller, K. -L. Kratz, M. Lewitowicz, S. M. Lukyanov, T. Mehren, A. C. Mueller, Yu. E. Penionzhkevich, F. Pougheon, M. G. Saint-Laurent, V. S. Salamatin, S. Shoedder, and A. Wöhr, Nucl. Phys. **A583**, 763 (1995).
[7] B. Vosicki, T. Bjornstad, L. C. Carraz, J. Heinemeier, and H. L. Ravn, Nucl. Instrum. Methods **186**, 307 (1981).
[8] A. Huck, G. Klotz, A. Knipper, C. Miehé, C. Richard-Serre, and G. Walter, in *Proceedings of the 4th International Conference on Nuclei Far from Stability, Helsingor, Denmark*, edited by P. G. Hansen and O. B. Nielsen, CERN Report No. 81-09 (1981), Vol. 2, p. 378.
[9] L. K. Fifield, M. A. C. Hotchkis, P. V. Drumm, T. R. Ophel, G. D. Putt, and D. C. Weisser, Nucl. Phys. **A417**, 534 (1984).
[10] R. L. Kozub, J. F. Shriner, Jr., M. M. Hindi, R. Holzmann, R. V. F. Janssens, T.-L. Khoo, W. C. Ma, M. Drigert, U. Garg, and J. J. Kolata, Phys. Rev. C **37**, R1791 (1988).
[11] D. P. Balamuth, U. J. Hüttmeier, and J. W. Arrison, Phys. Rev. C **48**, 2648 (1993).
[12] N. A. Jelley, K. H. Wilcox, R. B. Weisenmiller, G. J. Wozniak, and J. Cerny, Phys. Rev. C **9**, 2067 (1974).
[13] F. Maréchal, T. Suomijärvi, Y. Blumenfeld, A. Azhari, D. Bazin, J. A. Brown, P. D. Cottle, M. Fauerbach, T. Glasmacher, S. E. Hirzebruch, J. K. Jewell, J. H. Kelley, K. W. Kemper, P. F. Mantica, D. J. Morrissey, L. A. Riley, J. A. Scarpaci, H. Scheit, and M. Steiner, Phys. Rev. C **60**, 064623 (1999).
[14] J. A. Winger, P. F. Mantica, R. M. Ronningen, and M. A. Caprio, Phys. Rev. C **64**, 064318 (2001).
[15] J. A. Winger, P. F. Mantica, and R. M. Ronningen, in *Proceedings of the International Conference on Fission and Properties of Neutron-Rich Nuclei, Sanibel Island, FL (1998)*, edited by J. H. Hamilton and A. V. Ramayya (World Scientific, Singapore, 1998), p. 311.
[16] B. M. Sherrill, D. J. Morrissey, J. A. Nolen, Jr., and J. A. Winger, Nucl. Instrum. Methods B **56/57**, 1106 (1991).
[17] G. Audi, A. H. Wapstra, and C. Thibault, Nucl. Phys. **A729**, 337 (2003).
[18] G. Klotz, J. P. Gonidec, P. Baumann, and G. Walter, Nucl. Phys. **A197**, 229 (1972).
[19] E. K. Warburton and J. A. Becker, Phys. Rev. C **39**, 1535 (1989).
[20] C. L. Woods, Nucl. Phys. **A451**, 413 (1986).
[21] X. Ji and B. H. Wildenthal, Phys. Rev. C **39**, 701 (1989).
[22] B. A. Brown and B. H. Wildenthal, At. Data Nucl. Data Tables **33**, 347 (1985).
[23] B. A. Brown and B. H. Wildenthal, Nucl. Phys. **A474**, 290 (1987).
[24] I. S. Towner, Phys. Rep. **155**, 264 (1987).
[25] Ch. Miehé, Ph. Dessagne, P. Baumann, A. Huck, G. Klotz, A. Knipper, G. Walter, and G. Marguier, Phys. Rev. C **39**, 992 (1989).
[26] E. K. Warburton, Phys. Rev. C **44**, 268 (1991).
[27] P. M. Endt and R. B. Firestone, Nucl. Phys. **A633**, 1 (1998).
[28] J. A. Winger, H. H. Yousif, W. C. Ma, V. Ravikumar, W. Lui, S. K. Phillips, R. B. Piercey, P. F. Mantica, B. Pritychenko, R. M. Ronningen, and M. Steiner, in *Proceedings of the Second International Conference on Exotic Nuclei and Atomic Masses, Bel Aire, MI (1998)*, edited by B. M. Sherrill, D. J. Morrissey, and C. N. Davids (AIP Press, New York), p. 606.
[29] O. Sorlin, Zs. Dombrádi, D. Sohler, F. Azaiez, J. Timár, Yu.-E. Penionzhkevich, F. Amorini, D. Baiborodin, A. Bauchet, F. Becker, M. Belleguic, C. Borcea, C. Bourgeois, Z. Dlouhy, C. Donzaud, J. Duprat, L. Gaudefroy, D. Guillemaud-Mueller, F. Ibrahim, M. J. Lopez, R. Lucas, S. M. Lukyanov, V. Maslov, J. Mrazek, C. Moore, F. Nowacki, F. Pougheon, M. G. Saint-Laurent, F. Sarazin, J. A. Scarpaci, G. Sletten, M. Stanoiu, C. Stodel, M. Taylor, and C. Theisen, Eur. Phys. J. A **22**, 173 (2004).
[30] J. A. Cameron and B. Singh, Nucl. Data Sheets **92**, 783 (2001).